Effects of twin and surface facet on strain-rate sensitivity of gold nanowires at different temperatures

Chuang Deng and Frederic Sansoz[*]

School of Engineering and Materials Science Program, University of Vermont, Burlington, Vermont 05405, USA

We use classical molecular-dynamics simulations to examine the strain-rate sensitivity of single-crystalline and twinned Au nanowires (NWs) with a diameter of 12.3 nm deformed in tension at temperatures between 10 K and 450 K. It is found that the strain-rate sensitivity above 100 K is significantly smaller in twinned Au NWs with perfectly circular cross-section than in similar NWs without twins, while the activation volume remains in the same range of $1b^3 - 15b^3$ with b the magnitude of Burgers vector. This behavior is markedly different from that generally observed in bulk face-centered cubic metals where addition of nanoscale twins increases both strength and strain-rate sensitivity. Furthermore, our simulations show a threefold decrease in strain-rate sensitivity in twinned Au NWs with zigzag morphology constructed by assembly of {111} surface facets in comparison to the different types of circular Au NWs. The rate-controlling deformation mechanisms related to surface dislocation emission and twin-slip interaction, and their dependence on temperature and surface morphology are analyzed in detail. The combination of ultrahigh strength and decreased sensitivity to strain-rate predicted above 100 K in twinned Au NWs with faceted surface morphology holds great promise for creating metallic nanostructures with increased failure resistance to extreme loading conditions.

I. INTRODUCTION

The mechanical properties of face-centered cubic (FCC) metal nanowires (NWs), which are important building blocks of nanoscale devices, have been extensively studied in recent years using nanomechanical experiments[1–5] and molecular-dynamics (MD) simulations.[6–14] Past experimental studies[2,3,5] have proved that the yield strength of an FCC metal NW is markedly higher than that of its bulk counterpart due to size effects on plastic yielding. Several atomistic simulation studies[7,9,11–14] have also shown that added defects such as special surface facets and coherent twin boundaries (CTBs), can significantly influence the limit of elasticity and ultimate strength of FCC metal NWs. For instance, in a recent study, we have predicted by atomistic simulation that twinned Au NWs with zigzag {111} surface facets exhibit stronger size dependence on tensile yield strength than Au NWs with circular cross-section, which enabled us to predict near ideal strength in Au NWs under tensile deformation.[12] CTBs with a high degree of ordering and symmetry, and {111} surface facets have commonly been observed during the synthesis of FCC metal NWs.[3,4,14–17] To date, however, the predictions from MD simulations are difficult to verify experimentally because of the short simulation time scales (e.g., a few nanoseconds) and high strain-rates ($>10^6$ s^{-1}) involved in such simulations. Therefore, meaningful predictions from MD simulations can only be achieved successfully if strain-rate effects on NW properties are properly taken into account.

Zhu *et al.*[18] have proposed that activation volume, which is a measure of the number of atoms involved in a thermally activated process, provides a useful link between atomistic modeling and experiments, because this parameter can be determined from both methods. For thermally activated deformation processes in metals, the activation volume V^* is given by[19]

$$V^* = \sqrt{3}kT\frac{\partial \ln \dot{\varepsilon}}{\partial \sigma} = \frac{\sqrt{3}kT}{m\sigma}, \tag{1}$$

where k is the Boltzmann constant, T is the temperature, $\dot{\varepsilon}$ and σ are the strain-rate and uniaxial flow stress, respectively, and m is the strain-rate sensitivity which describes the power law relation between the yield stress and strain-rate, such as

$$\sigma = a\dot{\varepsilon}^m, \tag{2}$$

where a is a pre-exponential constant. Therefore, m can be calculated as

$$m = \frac{\partial \ln \sigma}{\partial \ln \dot{\varepsilon}}\bigg|_{\varepsilon,T} = \frac{\dot{\varepsilon}}{\sigma}\frac{\partial \sigma}{\partial \dot{\varepsilon}}. \tag{3}$$

The activation volume is an effective kinetic signature of deformation mechanism;[19–24] different rate-controlling mechanisms have different characteristic activation volumes. For instance, the activation volumes associated with lattice diffusion, surface assisted dislocation nucleation and bulk dislocation processes are in the range of $\sim 0.1b^3$, $1b^3 - 10b^3$, and $100b^3 - 1000b^3$, respectively, with b the magnitude of Burgers vector. In addition, the activation volume can be lowered by two orders of magnitude when the grain size of FCC metals is reduced from micrometer to nanometer scales due to strong grain size dependence on plasticity mechanisms.[19,20,22] Moreover, there have been experimental evidence showing that yield strength, ductility and strain-rate sensitivity in polycrystalline Cu films are significantly increased by introducing a high density of CTBs inside the grains.[24–30] For example, Lu *et al.*[29,30] have reported that m increases by one order of magnitude and V^* decreases from $1000b^3$ to only tens of b^3 when twins of 15 nm in size are added to bulk Cu samples of 200–300 nm in grain diameter.
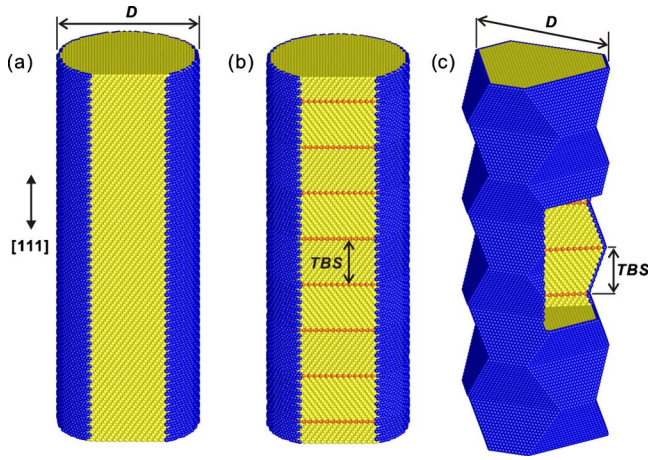
FIG. 1. (Color online) Atomistic models for [111]-oriented Au NWs with different types of microstructure. (a) Single-crystalline circular NW. (b) Twinned circular NW with (111) coherent twin boundaries and constant twin boundary spacing (TBS). (c) Twinned zigzag NW with {111} facets. All NWs have a diameter D = 12.3 nm. Some atoms have been removed to show the internal microstructure of each NW. Atom colors correspond to the local crystal structure according to Ackland and Jones' analysis (Ref. 33) (yellow=FCC; red=HCP; blue=surface atoms).

The present paper aims to characterize the influences of temperature and strain-rate on the ultimate strength and underlying deformation mechanisms of different types of Au NW with the presence of CTBs and different surface morphologies. To this end, classical MD simulations were used to determine the strain-rate sensitivity and activation volume of single crystalline and twinned Au NWs deformed under uniaxial loading in the temperature range of 10–450 K. The simulations predict that the strain-rate sensitivity of Au NWs can be dramatically reduced at temperatures above 100 K with the coupled effects of twinning and surface faceting.

II. SIMULATION METHODS

Classical MD simulations of Au NWs subjected to uniaxial tensile deformation were performed with LAMMPS (Ref. 31) using an embedded-atom method (EAM) potential for Au developed by Grochola *et al.*[32] Three types of microstructure in [111]-oriented Au NWs were simulated as shown in Fig. 1: single-crystalline circular NWs, twinned circular NWs, and twinned zigzag NWs with {111} surface facets. The method to construct the twinned zigzag structure can be found elsewhere.[11] The NW diameter (D) and twin boundary spacing (TBS) defined in Fig. 1 were 12.3 and 4.2 nm, respectively, in all NWs. Periodic boundary conditions were imposed along the [111] axis with a periodic length equal to 33.6 nm. All other directions were kept free. The models consisted of ~240,000 atoms. The time step was 5 fs. Each model was equilibrated under zero pressure for 100 ps in the isothermal-isobaric ensemble (constant number of particles, pressure and temperature, NPT) using a Nosé-Hoover thermostat. The NWs were deformed by straining the simulation box along the [111] direction at various rates from
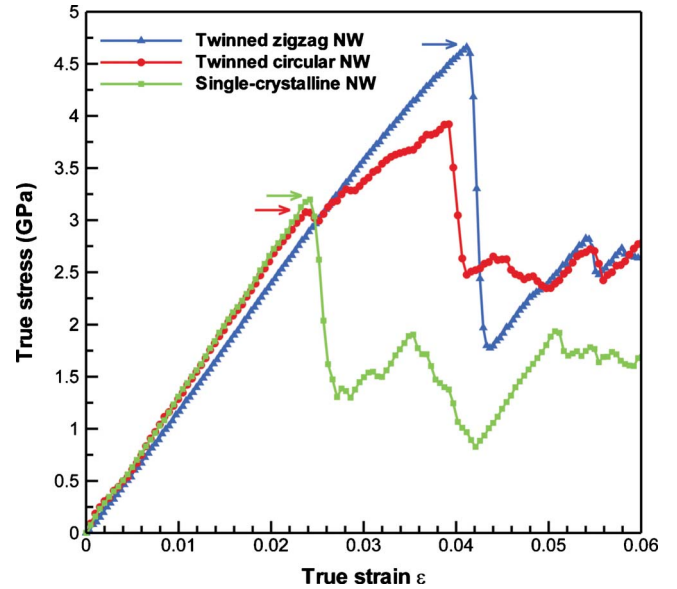

FIG. 2. (Color online) True stress-strain curves of Au NWs at 300 K deformed in tension at a strain-rate of 5×10^7 s^{-1}. Note that the twinned circular NW exhibits strong strain-hardening effect, which is markedly different from the sharp yielding behavior observed in the other types of NWs. The arrows show the limit of elasticity prior to the emission of the very first dislocations from the free surface.

5×10^6 s^{-1} to 1×10^9 s^{-1}. A Nosé-Hoover thermostat was used to maintain constant temperatures (ranging from 10 to 450 K) during the tensile deformation in canonical ensemble (constant number of particles, volume and temperature). The Ackland and Jones' analysis was used to determine the local crystal structure of atoms, such as FCC, body-centered cubic, hexagonal close-packed (HCP), or unknown, during deformation.[33] Stress in the direction of loading was calculated using the Virial theorem and averaged over the entire volume of the NW.[34]

III. RESULTS

A. Plastic behavior of Au NWs in tension

The stress-strain curves of Au NWs with different morphologies deformed at a tensile strain-rate of 5×10^7 s^{-1} and a temperature of 300 K are presented in Fig. 2. This figure shows that Au NWs subjected to tensile deformation exhibit two distinct types of plastic behavior in accordance with our previous reports using MD simulations at this temperature.[11,12] The first type of behavior was observed in single-crystalline circular NWs and twinned zigzag Au NWs, and corresponds to a quasibrittle behavior with an abrupt stress drop following the nucleation of the very first dislocations. This is similar to the mechanical behavior of defect-free gold whiskers subjected to tensile strain.[35] For these two materials the flow stress was directly measured at the stress value corresponding to the initial yield point. In contrast, in twinned circular Au NWs, significant strain-hardening effects resulting from the blockage of newly-emitted partial dislocations by CTBs were found at the initial yield point for
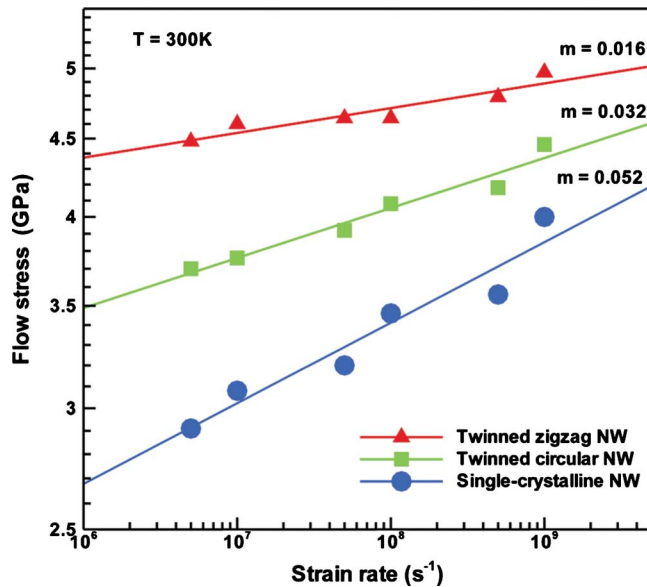
FIG. 3. (Color online) Flow stress as a function of tensile strain-rate in three types of Au NWs at 300 K.

FIG. 4. (Color online) Strain-rate sensitivity m as a function of temperature in three types of Au NWs deformed under tension.

temperatures larger than 100 K. Here, the flow stress was systematically higher than the yield stress, and therefore was determined by the maximum stress along the stress-strain curve.

B. Strain-rate sensitivity

Figure 3 presents the evolution of the flow stress as a function of tensile strain-rate determined from the stress-strain curves of all Au NWs studied at 300 K. This figure shows that, in a double-log graph, the flow stress linearly increases with the strain-rate for all NWs, which indicates that the strain-rate sensitivity m is constant over this range of strain-rates. It can also be mentioned that the levels of strain corresponding to the plastic flow stresses produced in Fig. 3 were almost constant in each NW, and equal to 0.043 ± 0.003, 0.041 ± 0.003, and 0.026 ± 0.003 for the twinned zigzag NWs, twinned circular NWs and single-crystal NWs, respectively, which therefore validates the use of Eq. (3) in the determination of m.

Furthermore, Fig. 3 reveals that the plastic behavior of circular Au NWs with nanoscale twins displays higher plastic flow stresses, as well as smaller strain-rate sensitivity ($m=0.032$) than that of circular ones without twins ($m=0.052$). It is also clearly shown in this figure that the addition of {111} surface facets to twinned NWs causes further increase in flow stress and decrease in strain-rate sensitivity ($m=0.016$) as compared to the different types of circular Au NWs.

The different evolutions of strain-rate sensitivity in the NW morphologies investigated are presented in Fig. 4 as a function of temperature. We can observe in this figure that the different values of strain-rate sensitivity calculated are in the range of 0.008–0.068 for temperatures between 10 and 450 K, which is in excellent agreement with the values measured experimentally ($m=0.035-0.046$) in bulk nanotwinned

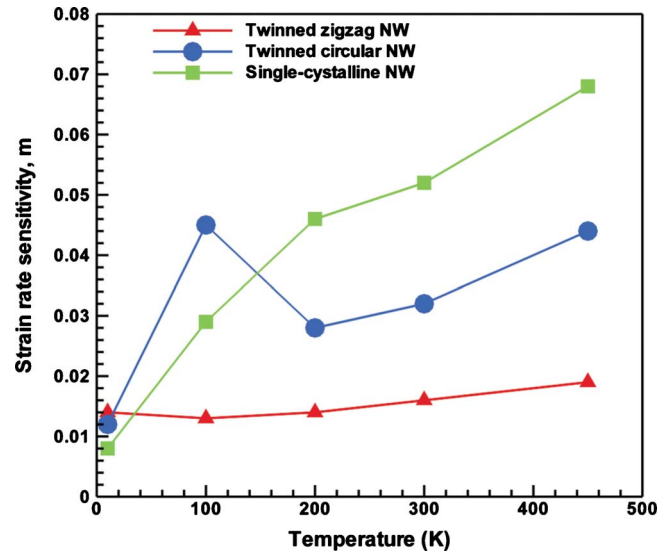Cu deformed at room temperature with $\dot{\varepsilon} < 10^{-2}$ s^{-1}.[27,28] Furthermore, we find that the zigzag Au NW with both CTBs and {111} surface facets shows dramatically smaller values of m than the two circular Au NWs for all temperatures except for 10 K. A weak dependence of m on temperature is also observed in the zigzag Au NW as m appears to remain quasiconstant at 0.0152 ± 0.0024 between 10 K and 450 K. In contrast, the strain-rate sensitivity of the single-crystalline circular Au NWs shows strong dependence on temperature as m monotonically increases from 0.008 to 0.068 when the temperature increases from 10 to 450 K. A peculiar behavior can also be found in the evolution of the strain-rate sensitivity of twinned circular Au NWs, which corresponds to higher sensitivity at $T \leq 100$ K and smaller one at $T > 100$ K, in comparison to that measured in the single-crystal NWs with no twins.

C. Deformation mechanisms

In order to characterize the influence of temperature on yielding mechanisms in different types of Au NWs, we present several snapshots of atomic-scale deformation in single-crystalline, twinned zigzag and twinned circular Au NWs after reaching the yield point at 10 and 300 K in Figs. 5–7, respectively. The deformation mechanisms in all Au NWs at 450 K (not shown) have also been examined, and were found to be identical to that at 300 K with only more noise due to thermal fluctuations.

Figures 5 and 6 clearly show that there is no change in deformation mode at yield point in single-crystalline and twinned zigzag Au NWs with varying temperature. More specifically, the yielding events take place via random surface nucleation of {111}⟨112⟩ Shockley partial dislocation in the single-crystalline NW, while the onset of plasticity in twinned zigzag NWs occurs by surface nucleation of {001}⟨110⟩ Lomer dislocations at specific sites where the CTBs intersect the free surface. Both types of slip mecha-
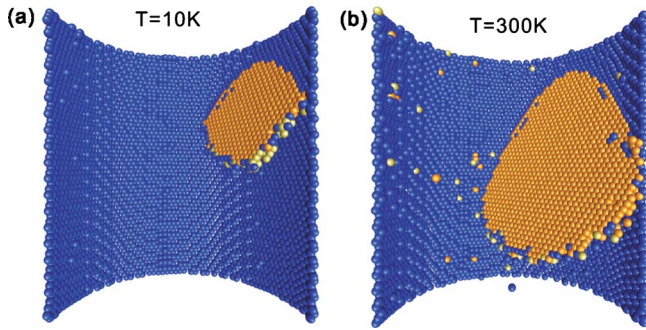
FIG. 5. (Color online) Snapshots of atomic-scale deformation at yield point in a single-crystalline Au NW under tensile loading at (a) 10 K and (b) 300 K. Atom colors correspond to the local lattice structure according to Ackland and Jones' analysis (Ref. 33) (yellow=HCP; blue=surface atoms). NW front and atoms in perfect FCC arrangement have been removed for clarity.

nism have already been reported at 300 K in previous atomistic studies,[11–13] which therefore confirms these predictions. It should also be noted that, in Fig. 6, the full dislocations emitted from the free surface are not blocked by the CTBs as opposed to the dislocations emitted in twinned circular Au NWs as shown below.

In contrast, different deformation mechanisms were found in twinned circular Au NWs as a function of temperature. For a model deformed at 10 K, the emitted Shockley partial dislocation, as shown in the right hand of Fig. 7(a), directly transmit from the parent grain through the CTB to form a full Lomer dislocation propagating on a (001) plane in the twin grain, which is accompanied with a sharp drop in stress. On the contrary, at 300 K, the partial dislocations emitted are immediately blocked by CTBs, as shown in Fig. 7(b), which gives rise to an increased flow stress and significant strain hardening effects. The maximum flow stress in twinned cir-
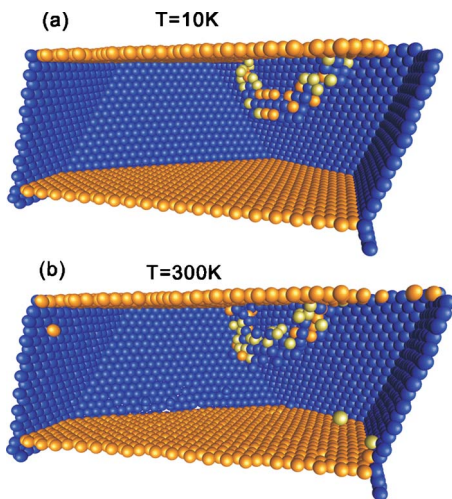

FIG. 6. (Color online) Snapshots of atomic-scale deformation at yield point in a twinned faceted Au NW under tensile loading at (a) 10 K and (b) 300 K. Atom colors correspond to the local lattice structure according to Ackland and Jones' analysis (Ref. 33) (yellow=HCP; blue=surface atoms). NW front and atoms in perfect FCC arrangement have been removed for clarity.
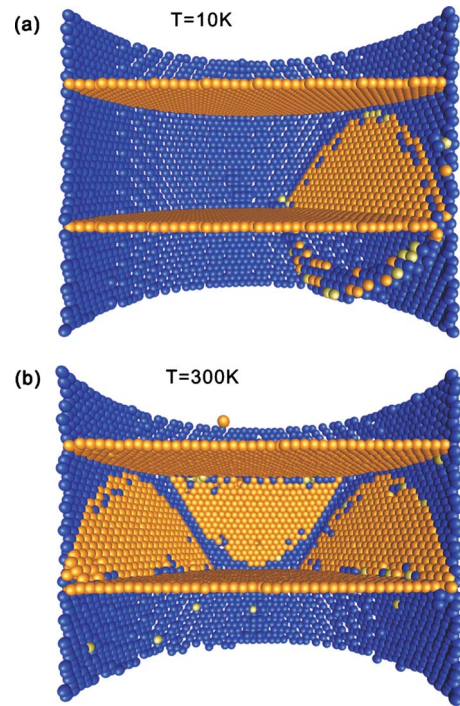

FIG. 7. (Color online) Snapshots of atomic-scale deformation in twinned circular Au NW at the maximum flow stress under tensile loading at (a) 10 K and (b) 300 K. Atom colors correspond to the local lattice structure according to Ackland and Jones' analysis (Ref. 33) (yellow=HCP; blue=surface atoms). NW front and atoms in perfect FCC arrangement have been removed for clarity. In (a), the partial dislocation can directly transmit through the CTB to form a full Lomer dislocation propagating on a {001} plane, while in (b) the partial dislocations are blocked by the CTBs.

cular Au NWs at 300 K is encountered when trailing partial dislocations are able to nucleate and propagate from the free surface to form full dislocations by recombination with the leading partials blocked at the CTBs. Subsequently, these full dislocations can be transmitted through the twin interfaces.[11]

D. Activation volume

The activation volumes calculated according to Eq. (1) by using the average of the maximum flow stresses at various strain-rates for all Au NWs are shown in Fig. 8 as a function of temperature. This figure shows that the activation volume of Au NWs monotonically increases with the temperature, which just confirms that more atoms are involved in the plastic deformation process at higher temperatures. The activation volumes of single-crystalline and twinned circular Au NWs are found to be close in Fig. 8, which is due to the fact that the mode of plastic deformation in both NW types is controlled by the same mechanism, i.e., surface nucleation of Shockley partial dislocations, as shown in Figs. 5 and 7. The predicted activation volumes are all in the range $1b^3 - 15b^3$, which agrees well with that for the surface nucleation of partial dislocations in Cu NWs ($1b^3 - 10b^3$) reported by Zhu et al.[36] from calculations using the free-end nudged elastic band method.
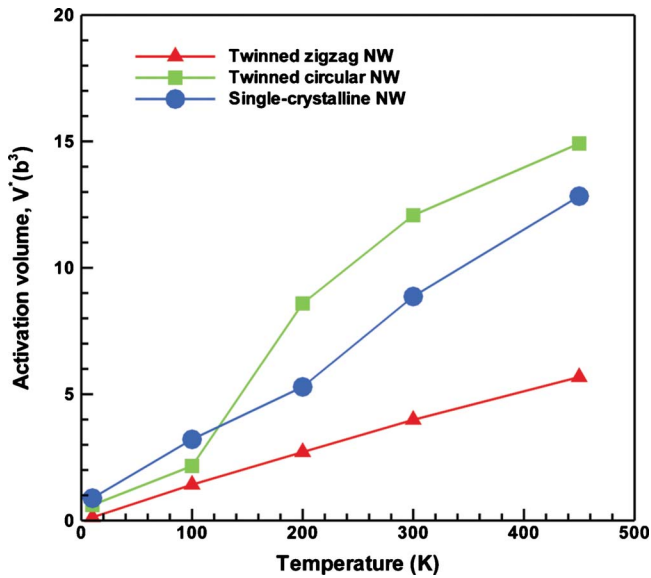
FIG. 8. (Color online) Activation volume as a function of temperature in three types of Au NWs.

Figure 8 also shows that the activation volumes predicted in twinned zigzag Au NWs are $V^* = 1b^3 - 5b^3$ in the temperature range of 10–450 K, which indicates that V^* is slightly smaller than that predicted in circular Au NWs for all temperatures. However, this change in activation volume is not significant enough to be attributed to a different rate-controlling deformation mechanism. Instead, we can assume that it is related to the change in dislocation character from the emission of partial dislocations ($b = 0.166$ nm) to that of full $\{001\}\langle 110 \rangle$ dislocations ($b = 0.288$ nm) between circular NWs and zigzag NWs, respectively.

IV. DISCUSSION

A. Role of twinning and surface morphology on rate sensitivity of Au NWs

All experimental observations made in the past on bulk Cu samples tested at room temperature with small strain-rates ($\dot{\varepsilon} < 10^{-2}$ s^{-1}) have proved that the addition of nanoscale CTBs in this type of metal causes a pronounced increase in strength, tensile ductility and strain-rate sensitivity.[20,25–30] For example, it was found that m varies by almost an order of magnitude from $m = 0.005$ to 0.043 in Cu samples of 200–300 nm in mean grain size by adding twins of 15 nm in spacing using pulsed electrodeposition.[27] It was also found that such an increase in strain-rate sensitivity was accompanied by a decrease in activation volume, which indicated a fundamental change in rate-controlling deformation mechanism with decreasing twin size. Atomistic simulations have suggested that strengthening and strain-rate sensitivity effects in twinned Cu films result from a shift from bulk forest-dislocation activity without twins to complex mechanisms of transmission of dislocations through CTBs.[37] Similarly, it was shown by atomistic simulations that the addition of nanoscale twins to Au pillars deformed in compression causes the slip activity to change from easy dislocation glide

to slip arrest in the form of Lomer-Cottrell locks at the intersection of partial dislocations and pre-existing twin boundaries, which largely depends upon the spacing between the twin lamellas.[38] Lu and co-workers[29,30] have also recently proposed a mechanistic model to correlate the activation volume and rate-controlling deformation mechanism in bulk nanocrystalline and nanotwinned Cu to the reciprocal of the square root of grain size and twin boundary spacing using a classical Hall-Petch relationship. This model predicts that decreasing twin spacing or grain size results in decreasing V^* and increasing m values.

The present simulation study, however, shows that the influence of nanoscale twinning on strain-rate sensitivity in crystalline Au NWs deformed in tension at $T > 100$ K is contrary to that commonly observed experimentally in bulk Cu samples at room temperature, i.e., the addition of CTBs acts to decrease the strain-rate sensitivity of Au NWs. By way of illustration, we have found here that the sensitivity predicted in twinned circular Au NWs at 300 K decreases by 38% (from $m = 0.052$ to 0.032) with respect to a Au NW of identical geometry with no twins. Our study also shows that the activation volume does not significantly change between the different NW morphologies, which suggests that all Au NWs are subject to the same rate-controlling deformation mechanism whether CTBs exist or not. It is essential to note that, while emitted partial dislocations are all blocked by CTBs in twinned circular Au NWs at $T > 100$ K, the plastic yielding mechanism is found to be the surface emission of leading and trailing dislocations. These results therefore points to the conclusion that in Au NWs the rate-controlling deformation mechanism corresponds to the emission of dislocations from free surfaces as opposed to the transmission of dislocations through CTBs, because twin-CTB reactions do not take place before the peak stress in the stress-strain curves. Zhu et al.[36] and Hirel et al.[39,40] have also demonstrated earlier the dependence of surface dislocation emission on strain-rate and temperature in perfectly crystalline metal NWs and thin films, respectively.

Furthermore, the results predicted in twinned zigzag Au NWs strongly support the idea that the predominant deformation mechanism controlling the rate of plastic flow in Au NWs is mediated by the free surface. When the surface morphology is varied from circular to zigzag with $\{111\}$ facets, the nature of dislocation emission at the intersection of CTBs with the free surface changes from partial dislocations to full Lomer dislocations on $\{001\}$ planes. Here the decrease in strain-rate sensitivity in twinned faceted structures could be attributed to the stress concentration at the intersection between CTBs and the free surface, which causes the dislocation emission to occur at specific sites, as opposed to random sites in crystalline NWs with no twins.

Therefore, a major conclusion of this work is that CTBs in combination with $\{111\}$ surface facets can be utilized to further increase tensile strength in realistic Au NWs, while decreasing their sensitivity to strain-rate at $T > 100$ K. In particular, Figs. 2–4 show that twinned faceted Au NWs are both the strongest and least sensitive to strain-rate with $m = 0.0152 \pm 0.0024$ between 10 and 450 K, which corresponds to a 71% decrease in m as compared to the value in twin-free Au NWs. It could also be inferred that at significantly lower

strain-rates (e.g., 10^{-2} s^{-1}, which is typical for experimental studies), twinned faceted Au NWs might exhibit superior mechanical behavior with a combination of high strength and low sensitivity to strain-rate, compared to other types of Au NWs.

B. Temperature-dependence of plastic flow in Au NWs

Our simulations did not show any change in deformation mechanism as a function of temperature between 10 and 450 K in single-crystal and twinned zigzag Au NWs. However, two deformation mechanisms in twinned circular Au NWs were revealed in Fig. 7 depending on the temperature. At 10 K, the Shockley partial dislocations emitted from the free surface were found to be directly transmitted through CTBs after the yield point, while at 300 K these dislocations were immediately blocked by CTBs at the early stage of plastic deformation. In a previous study,[41] we have shown that the blockage of Shockley partial dislocations at CTBs in twinned FCC metal NWs depends on the relative value of stress required to nucleate a new dislocation (σ_N) with respect to the resistance stress from CTBs to stop a glide dislocation (σ_R), i.e., dislocation blockage takes place when $\sigma_N < \sigma_R$. In the present study, we have calculated the dislocation nucleation stress σ_N in twinned circular Au NWs at different temperatures ranging from 10 to 450 K by using the method explained in Sec. II for a tensile strain-rate of 5×10^7 s^{-1}. Similarly, we have determined the resistance stresses from CTBs on glide dislocation (σ_R) at the same temperatures by employing the model described in Ref. 41, which enabled us to calculate the tensile stress required for a pre-existing Shockley partial dislocation to transmit through a CTB in a bulk cubic model loaded along the [111] direction. The values of σ_N, σ_R, and the maximum flow stress σ_F are plotted as a function of temperature in Fig. 9 for comparison. While all the stresses (σ_N, σ_R, and σ_F) shown in this figure decrease at elevated temperatures, the decrease in σ_N and σ_F with increasing temperature is more pronounced than that for σ_R. Consequently, Fig. 9 reveals the existence of a critical temperature at 100 K where $\sigma_N = \sigma_R$. This temperature therefore marks the lower limit in temperature where CTBs are able to block partial dislocations emitted from the free surface in twinned circular Au NWs. This result is in excellent agreement with the deformation modes of twinned Au NWs shown in Figs. 7(a) and 7(b).

This change in deformation mechanism as a function of temperature may also explain the peculiar behavior in terms of strain-rate sensitivity observed in Fig. 4. It was found in this figure that the strain-rate sensitivity becomes higher in twinned circular NWs than in single-crystal NWs when $T \leq 100$ K and *vice versa* when $T > 100$ K. It can be assumed that the rate-controlling deformation mechanism in twinned circular NWs always corresponds to surface-assisted dislocation emission for $T = 10$ K ~ 450 K, despite the fact that CTBs are no longer effective barrier to dislocation motion when $T \leq 100$ K. More specifically, for $T \leq 100$ K, the plastic flow is controlled by the mechanism of emission of leading partials only as these can easily transmit through the CTBs in this low-temperature regime [Fig. 7(a)]. On the con-
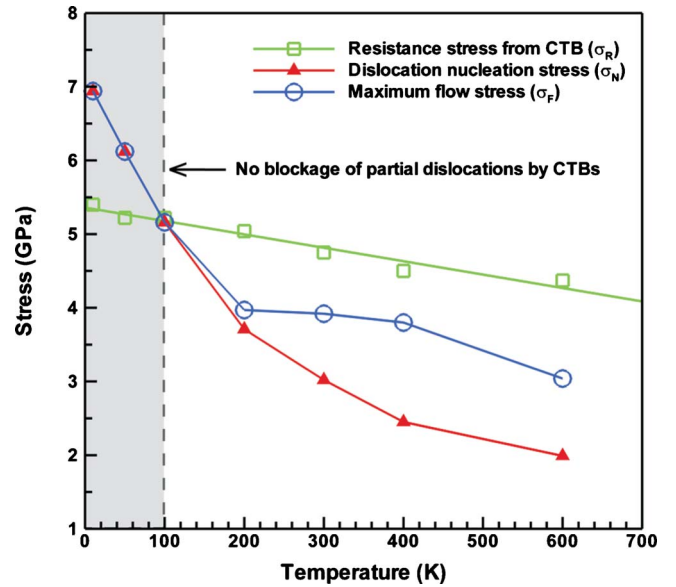

FIG. 9. (Color online) Resistance stress from CTBs to stop dislocation glide (σ_R), stress required to emit new surface dislocations (σ_N) and maximum flow stress (σ_F) in twinned circular Au NWs as a function of temperature.

trary, for $T > 100$ K the rate-controlling mechanism shifts to the emission of the trailing partials, because a trailing partial has to recombine with a leading partial blocked at a CTB to result in full dislocation transmission through the twin interface [Fig. 7(a)]. While the origin of differences in strain-rate sensitivity caused by surface emission of either leading or trailing partials is unclear, we can conclude that the rate-controlling mechanisms in Au NWs with CTBs are different from that in bulk Cu with CTBs, which are dominated by CTB-mediated slip transfers.

V. CONCLUSIONS

We have studied the influence of CTBs and {111} surface facets on the strain-rate sensitivity of Au NWs under uniaxial tensile deformation at temperatures between 10 and 450 K by classical MD simulations. The rate-controlling mechanisms were confirmed to be dominated by surface-assisted dislocation emission in all Au NWs regardless the microstructure. However, it was found that the addition of CTBs can significantly lower the strain-rate sensitivity in circular Au NWs at $T > 100$ K. This result is in stark contrast to that in bulk metals where the addition of nanoscale CTBs generally leads to substantial increase in strain-rate sensitivity. Moreover, we have observed a marked increase in tensile strength and a considerable decrease in strain-rate sensitivity in twinned Au NWs by introducing {111} surface facets. Our findings therefore demonstrate strong coupled effects of surface morphology and internal microstructure on the increase in mechanical strength and the reduction in strain-rate sensitivity in metal NWs. This theoretical work should also encourage experimental studies in the areas of nanowire mechanics and nanoscale interfacial plasticity.

*frederic.sansoz@uvm.edu

[1] X. Li, H. Gao, C. J. Murphy, and K. K. Caswell, Nano Lett. **3**, 1495 (2003).

[2] B. Wu, A. Heidelberg, and J. J. Boland, Nature Mater. **4**, 525 (2005).

[3] B. Wu, A. Heidelberg, and J. J. Boland, Nano Lett. **6**, 468 (2006).

[4] S. Zhong, T. Koch, M. Wang, T. Scherer, S. Walheim, H. Hahn, and T. Schimmel, Small **5**, 2265 (2009).

[5] G. Richter, K. Hillerich, D. S. Gianola, R. Monig, O. Kraft, and C. A. Volkert, Nano Lett. **9**, 3048 (2009).

[6] K. Gall, J. Diao, and M. L. Dunn, Nano Lett. **4**, 2431 (2004).

[7] B. Hyde, H. D. Espinosa, and D. Farkas, JOM **57**, 62 (2005).

[8] H. S. Park, K. Gall, and J. A. Zimmerman, J. Mech. Phys. Solids **54**, 1862 (2006).

[9] A. M. Leach, M. McDowell, and K. Gall, Adv. Funct. Mater. **17**, 43 (2007).

[10] V. Dupont and F. Sansoz, J. Mater. Res. **24**, 948 (2009).

[11] C. Deng and F. Sansoz, Nano Lett. **9**, 1517 (2009).

[12] C. Deng and F. Sansoz, ACS Nano **3**, 3001 (2009).

[13] C. Deng and F. Sansoz, Appl. Phys. Lett. **95**, 091914 (2009).

[14] Y. Zhang and H. Huang, Nanoscale Res. Lett. **4**, 34 (2009).

[15] M. Tian, J. Wang, J. Kurtz, T. E. Mallouk, and M. H. W. Chan, Nano Lett. **3**, 919 (2003).

[16] J. Wang, M. Tian, T. E. Mallouk, and M. H. W. Chan, J. Phys. Chem. B **108**, 841 (2004).

[17] A. Halder and N. Ravishankar, Adv. Mater. **19**, 1854 (2007).

[18] T. Zhu, J. Li, S. Ogata, and S. Yip, MRS Bull. **34**, 167 (2009).

[19] R. J. Asaro and S. Suresh, Acta Mater. **53**, 3369 (2005).

[20] Q. Wei, S. Cheng, K. T. Ramesh, and E. Ma, Mater. Sci. Eng., A **381**, 71 (2004).

[21] Y. M. Wang, A. V. Hamza, and E. Ma, Acta Mater. **54**, 2715 (2006).

[22] R. W. Armstrong and P. Rodriguez, Philos. Mag. **86**, 5787 (2006).

[23] J. Monk and D. Farkas, Phys. Rev. B **75**, 045414 (2007).

[24] R. J. Asaro and Y. Kulkarni, Scr. Mater. **58**, 389 (2008).

[25] L. Lu, Y. Shen, X. Chen, L. Qian, and K. Lu, Science **304**, 422 (2004).

[26] O. Anderoglu, A. Misra, H. Wang, F. Ronning, M. F. Hundley, and X. Zhang, Appl. Phys. Lett. **93**, 083108 (2008).

[27] Y. F. Shen, L. Lu, M. Dao, and S. Suresh, Scr. Mater. **55**, 319 (2006).

[28] M. Dao, L. Lu, Y. F. Shen, and S. Suresh, Acta Mater. **54**, 5421 (2006).

[29] L. Lu, M. Dao, T. Zhu, and J. Li, Scr. Mater. **60**, 1062 (2009).

[30] L. Lu, T. Zhu, Y. Shen, M. Dao, K. Lu, and S. Suresh, Acta Mater. **57**, 5165 (2009).

[31] S. J. Plimpton, J. Comput. Phys. **117**, 1 (1995).

[32] G. Grochola, S. P. Russo, and I. K. Snook, J. Chem. Phys. **123**, 204719 (2005).

[33] G. J. Ackland and A. P. Jones, Phys. Rev. B **73**, 054104 (2006).

[34] J. Diao, K. Gall, and M. L. Dunn, J. Mech. Phys. Solids **52**, 1935 (2004).

[35] S. S. Brenner, J. Appl. Phys. **30**, 266 (1959).

[36] T. Zhu, J. Li, A. Samanta, A. Leach, and K. Gall, Phys. Rev. Lett. **100**, 025502 (2008).

[37] T. Zhu, J. Li, A. Samanta, H. G. Kim, and S. Suresh, Proc. Natl. Acad. Sci. U.S.A. **104**, 3031 (2007).

[38] K. A. Afanasyev and F. Sansoz, Nano Lett. **7**, 2056 (2007).

[39] P. Hirel, S. Brochard, L. Pizzagalli, and P. Beauchamp, Scr. Mater. **57**, 1141 (2007).

[40] P. Hirel, S. Brochard, L. Pizzagalli, and P. Beauchamp, Phys. Rev. B **78**, 064109 (2008).

[41] C. Deng and F. Sansoz, Acta Mater. **57**, 6090 (2009).